MATERIAL CLASSIFICATION USING PASSIVE POLARIMETRIC IMAGERY

Vimal Thilak, Charles D. Creusere and David G. Voelz

Klipsch School of Electrical and Computer Engineering
New Mexico State University
Las Cruces, NM 88003, USA
Email: {vimal, ccreuser, davvoelz}@nmsu.edu

ABSTRACT

Passive imaging polarimetry has emerged as an useful tool in many remote sensing applications including material classification, target detection and shape extraction. In this paper we present a method to classify specular objects based on their material composition from passive polarimetric imagery. The proposed algorithm is built on an iterative model-based method to recover the complex index of refraction of a specular target from multiple polarization measurements. The recovered parameters are then used to discriminate between objects by employing the nearest neighbor rule. The effectiveness of the proposed method is validated with data collected in laboratory conditions. Experimental results indicate that the classification approach is highly effective for distinguishing between various targets of interest. Most significantly, the proposed classification method is robust to a wide range of observational geometry.

Index Terms— remote sensing, illumination invariant object recognition, passive polarimetry, material classification, Stokes vector

1. INTRODUCTION

Polarization is a property of light or electromagnetic radiation that conveys information about the orientation of the transverse electric and magnetic fields. The polarization of reflected light complements other electromagnetic radiation attributes such as intensity, frequency, or spectral characteristics. This makes polarization a useful tool in many remote sensing applications including material classification [1, 2], shape extraction [3], target detection and recognition [4].

Material classification and recognition in uncontrolled environments is an important task in remote sensing applications such as target recognition, image segmentation and shape extraction as well as in industrial inspection. The utility of passive polarimetry for material classification was first demonstrated by Wolff [1]. He showed it was possible to distinguish between metals and dielectrics by recording the polarization state of specularly reflected light using a passive polarimeter. His method involves a threshold-based discrimination procedure that relies on the polarization Fresnel ratio [1], the ratio of perpendicular to parallel polarization state components. More recently, Zallat, Grabbling and Takakura [2] have proposed a clustering-based approach for material classification using passive polarimetric imagery.

In this paper we present a material classification algorithm for specular targets in passive polarimetric imagery that is robust to illumination conditions. This method uses an iterative model-based approach [5] to estimate the complex index of refraction of specular targets from multiple polarization measurements. The extracted index of refraction thus forms a feature vector to which we apply the well known nearest neighbor algorithm [6] for classification. The proposed method is applicable to a wide class of objects that are of interest in remote sensing applications unlike the method of [1] which is applicable only to purely specular objects. In particular, the proposed approach enables us to distinguish between metals like copper and aluminum as well as painted surfaces.

2. PROBLEM DESCRIPTION

Fig. 1 illustrates the assumed observational geometry. The objective here is to first recover the complex index of refraction of the object from multiple polarization measurements which is then used to classify targets. θ_{i1} and θ_{i2} denote the incident zenith angle with respect to the surface normal $\tilde{\mathbf{z}}$ corresponding to two different positions of the illumination source. θ_r is the view angle or the reflected zenith angle with respect to the surface normal $\tilde{\mathbf{z}}$, θ_{sc1} and θ_{sc2} are the angles between the source and the camera corresponding to the two different locations of the source. Furthermore, it is assumed that the source is unpolarized and that the camera is fixed and is in the plane of incidence.

The object is also assumed to be planar and to have a rough surface which is modeled as a collection of microfacets, a model referred to as the microfacet model in literature [7]. This model does not account for volumetric scattering; thus,

The authors thank the National Geospatial-Intelligence Agency for supporting this work through grant number HM1581-04-C-2-2029.

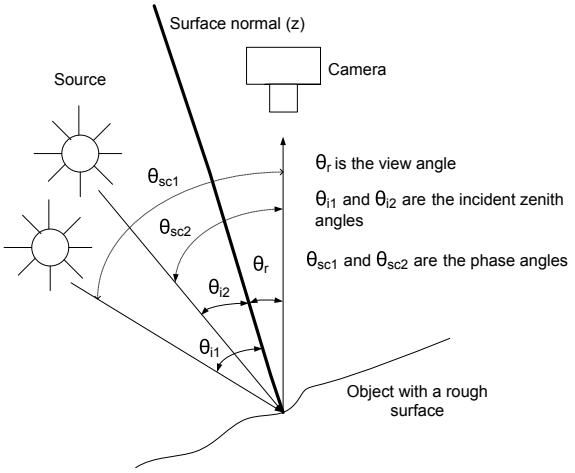

Fig. 1. Geometry assumed for the index of refraction estimation.

the optical scattering is assumed to be caused entirely by specular scattering.

3. POLARIMETRIC BIDIRECTIONAL REFLECTANCE DISTRIBUTION FUNCTION

The BRDF characterizes optical scattering from surface reflections and is given by

$$f(\theta_i, \phi_i, \theta_r, \phi_r, \lambda) = \frac{dL_r(\theta_r, \phi_r)}{dE(\theta_i, \phi_i)} sr^{-1} \tag{1}$$

where L_r is the radiance leaving the surface with units watts per square meter per steradian $\frac{W}{m^2 - sr}$, E is the irradiance incident on the surface with units watts per square meter $\frac{W}{m^2}$. This results in the BRDF having units of inverse steradians sr^{-1}. Most materials have azimuthal or rotational symmetry about the surface normal. Hence the azimuthal angle can be expressed as a difference between ϕ_r and ϕ_i, $\phi = \phi_r - \phi_i$, which reduces the degrees of freedom by one. In addition, we assume that the polarimetric measurements are made in the visible region of the spectrum which allows us to drop the argument λ. Thus, the BRDF is seen to be a function of three variables and is denoted by $f(\theta_i, \theta_r, \phi)$.

The polarimetric BRDF (pBRDF) is a generalization of the scalar BRDF that also models polarization as well. The pBRDF can be formally written as

$$d\mathbf{L_r}(\theta_r, \phi_r) = \mathbf{F}(\theta_i, \theta_r, \phi_r - \phi_i) d\mathbf{E}(\theta_i, \phi_i) \tag{2}$$

where $\mathbf{F}$ is the pBRDF Mueller matrix, $\mathbf{L_r}$ is the reflected Stokes vector and $\mathbf{E}$ is the incident Stokes vector.

In this paper, we utilize the pBRDF model proposed by Priest and Meier [7]. This model can characterize the specular component of scattering for a wide variety of target materials, for example aluminum and paints [8], that are of interest in remote sensing applications. We present the pBRDF equations necessary for our work in the next section and refer the interested reader to [7] for additional details.

3.1. Polarimetric BRDF for the microfacet model

The microfacet model assumes that a rough surface is composed of a collection of microfacets. Each individual microfacet is assumed to be a specular reflector obeying Fresnel's equations [8]. Furthermore, the volumetric scattering is assumed to be completely depolarizing. Thus, the optical scattering is caused only by surface or specular scattering. With these assumptions, the expression for the pBRDF Mueller matrix is given by [7]

$$f_{jl}(\theta_i, \theta_r, \phi_r - \phi_i) = \frac{m_{jl}(\theta_i, \theta_r, \phi_r - \phi_i)}{8\pi\sigma^2 \cos^4(\theta)} \frac{\exp\left[-\frac{\tan^2(\theta)}{2\sigma^2}\right]}{\cos(\theta_r)\cos(\theta_i)} \tag{3}$$

where f_{jl} denotes the element in the j^{th} row and l^{th} column of the pBRDF Mueller matrix $\mathbf{F}$, m_{jl} denotes the element in the j^{th} row and l^{th} column of the Fresnel reflectance Mueller matrix $\mathbf{M}$, θ is the angle of orientation of the microfacets relative to the mean surface normal and σ describes the surface roughness. The angle of orientation of the microfacets relative to the mean surface normal is given by

$$\theta = \arccos\left(\frac{\cos(\theta_i) + \cos(\theta_r)}{2\cos(\beta)}\right) \tag{4}$$

where

$$\cos(2\beta) = cos(\theta_i)cos(\theta_r) + sin(\theta_i)sin(\theta_r)cos(\phi_r - \phi_i) \tag{5}$$

The model given by (3) has three parameters namely n, k and σ where n and k are the real and imaginary parts of the index of refraction while σ is the surface roughness parameter. For our work, we assume that the amount of circular polarization in the reflected signal is insignificant, which is consistent with the general understanding of most naturally illuminated surfaces [8]. This assumption reduces $\mathbf{F}$ and $\mathbf{M}$ to 3×3 matrices. Explicit expressions for all the elements of the Fresnel reflectance matrix $\mathbf{M}$ are provided by Priest and Meier [7].

3.2. The microfacet pBRDF for scattering in the plane of incidence

The polarimetric BRDF equation simplifies in the case of scattering in the plane of incidence where $\phi_r - \phi_i = 180°$. In this case the Fresnel reflectance Mueller matrix $\mathbf{M}$ is given by

$$\mathbf{M} = \begin{pmatrix} m_{00} & m_{10} & 0 \\ m_{10} & m_{00} & 0 \\ 0 & 0 & m_{22} \end{pmatrix} \tag{6}$$

where we have dropped the arguments for the individual elements of $\mathbf{M}$ for the sake of convenience. The pBRDF Mueller matrix $\mathbf{F}$ is therefore defined by (3) and (6).

4. DERIVING THE DEGREE OF POLARIZATION FROM THE MIRCROFACET PBRDF MODEL

In this section an expression for the degree of polarization (DOP) is derived for the case of scattering in the plane of incidence. The illumination source is assumed to be unpolarized which is the case in passive remote sensing systems. Thus the input Stokes vector is given by $[1 \;\; 0 \;\; 0]^t$ where t denotes the vector transposition operator. In the following we drop the arguments for the individual elements f_{jl} for convenience. Assuming that the zenith angles for the source and the camera are θ_i and θ_r respectively, the observed Stokes vector at the camera can be shown to be [5]

$$\begin{pmatrix} s_0^r \\ s_1^r \\ s_2^r \end{pmatrix} = \begin{pmatrix} f_{00} \\ f_{10} \\ 0 \end{pmatrix} \tag{7}$$

where the superscript r denotes the Stokes vector components for reflected light. The degree of polarization of the observed Stokes vector is given by

$$P = \frac{m_{10}}{m_{00}} \tag{8}$$

which follows from (3).

The degree of polairzation given by (8) can be further simplified as shown in [5] to

$$P\left(n,k,\beta\right) = \frac{2A\sin^2(\beta)\cos(\beta)}{A^2\cos^2(\beta) + \sin^4(\beta) + B^2\cos^2(\beta)} \tag{9}$$

where n and k are the real and imaginary parts of the complex index of refraction and β is given by

$$\beta = \frac{\theta_i + \theta_r}{2} \tag{10}$$

or

$$\beta = \frac{\theta_{sc}}{2} \tag{11}$$

from fig. 1. The quantities A and B are defined as:

$$A = \sqrt{\frac{\sqrt{C} + D}{2}} \tag{12}$$

and

$$B = \sqrt{\frac{\sqrt{C} - D}{2}} \tag{13}$$

where

$$C = 4n^2k^2 + D^2 \tag{14}$$

and

$$D = n^2 - k^2 - \sin^2(\beta). \tag{15}$$

5. COMPLEX INDEX OF REFRACTION ESTIMATION

The objective is to recover the index of refraction from multiple degree of polarization measurements. We observe from (9) that the DOP is a function of n, k, θ_i and θ_r. If θ_{sc} is known, then it follows from (9) that the DOP is a function of the index of refraction. The assumption that the phase angle θ_{sc} is known at the camera is not unreasonable in many remote sensing applications given that the imaging platform is likely to have a GPS on board and is thus able estimate the position of the illumination source, for example the Sun, relative to its own position with high accuracy. Thus, the complex index of refraction can be estimated by using (9) by making multiple DOP measurements with the source at different positions. By collecting multiple measurements we have a system of nonlinear equations given by

$$P_j\left(n,k\right) = \frac{2A_j\sin^2(\beta_j)\cos(\beta_j)}{A_j^2\cos^2(\beta_j) + \sin^4(\beta_j) + B_j^2\cos^2(\beta_j)} \tag{16}$$

where $j \in \{1, 2, \cdots T\}$. Assuming $T \geq 3$, it is easy to see that the (16) corresponds to an overdetermined system of nonlinear equations. Thus, the system can be recast as a nonlinear least squares problem, which is solved using the well known Levenberg-Marquardt method as described in [5].

6. MATERIAL CLASSIFICATION

Target objects are classified into different categories based on their extracted index of refraction. The index of refraction is a fundamental parameter that describes a material and is thus naturally suited for material classification. In this paper, we use the well known nearest neighbor method [6] with the Euclidean distance metric for classification. This method classifies a test vector by assigning it to the class associated with the nearest prototype in the training set.

7. EXPERIMENTAL RESULTS

The proposed classification method is validated by using data collected under laboratory conditions. The polarization measurements are collected with a passive imagining polarimeter developed by the Electro-Optics Research Lab (EORL) [9] at New Mexico State University. The EORL polarimeter consists of a linear polarizer mounted in a rotation stage, a spectral filter (center wavelength of 650nm and a bandwidth of 80 nm for the results shown here) and a scientific-grade camera. A tungsten filament light source provides the illumination in our experiments. The Stokes vector images are acquired by taking several images of a scene with the polarizer at a different orientation for each measurement. The interested reader is referred to [9] for additional details regarding the EORL polarimeter.

Table 1. Experimental results for the training set. The view angle is 60°. n, k denote the reference index of refraction values obtained from [8, 10] while $\widehat{n}$ and $\widehat{k}$ denote the estimates.

Material	Angle of Incidence ($^\circ$)	n	k	$\widehat{n}$	$\widehat{k}$
Green paint	40-80	1.39	0.34	1.47	0.47
Aluminum	35-80	1.24	6.60	1.64	4.56
Copper	35-70	0.4	2.95	0.54	3.19

Table 2. Experimental results for the test aluminum sample. The angle of incidence was varied from 35° to 80°.

View Angle ($^\circ$)	$\widehat{n}$	$\widehat{k}$	Classification result
60	1.37	3.97	Aluminum
50	1.60	4.34	Aluminum

A Styrofoam piece coated with flat green paint, a piece of roughened copper and a piece of roughened aluminum were considered as the reference objects while a second piece of roughened aluminum was used as the test object. The degree of polarization (DOP) values needed for estimation were computed by averaging at least 100 by 100 pixels in the Stokes vector images. Table 1 shows the estimates obtained for the training set. The measurements for the training set were made with the view angle fixed at 60°. The index of refraction values published in literature [8, 10] have also been included in table 1 for comparison. We note here that for the copper target, the iterative algorithm converged to the desired solution for a narrower range of the angles of incidence compared to aluminum and green paint. This may be because the copper target is more specular than the aluminum or green paint target. Consequently, the specular lobe of the copper piece must be narrower than that of the other targets considered in this study.

Table 2 lists the estimates for the test sample as well as the classification results. Table 2 also shows that the classification method assigns the test sample to the appropriate class (aluminum) correctly in both the cases considered in our experiments. More importantly, it is seen that the index of refraction can be a useful feature vector for performing material classification that is robust to illumination conditions.

8. CONCLUSION

In this paper we present a method to classify specular objects based on their material composition from passive polarimetric imagery. The proposed algorithm is built on an iterative model-based method to recover the complex index of refraction of a specular target from multiple passive polarization measurements. The extracted parameters are used as inputs for the nearest neighbor method to discriminate between objects. Experimental results with laboratory data indicate that the classification approach is highly effective for distinguishing between various targets of interest. The proposed classification method is robust to a wide range of illumination conditions considered in our experiments. Current and future work involved considering more observational geometries for experimental data collection as well as other targets of interest in our experiments.

9. REFERENCES

[1] L. B. Wolff, "Polarization-based material classification from specular reflection," *IEEE Trans. on Pattern Anal. Mach. Intell.*, vol. 12(11), pp. 1059–1071, 1990.

[2] J. Zallat, P. Grabbling, and Y. V. Takakura, "Using polarimetric imaging for material classification," *Proc. 2003 International Conf. on Image Processing*, vol. 2, pp. II– 827–30 vol.3, 2003.

[3] D. Miyazaki, M. Kagesawa, and K. Ikeuchi, "Transparent surface modeling from a pair of polarization images," *IEEE Trans. on Pattern Anal. Mach. Intell.*, vol. 26(11), pp. 73–82, 2004.

[4] F. Goudail, P. Terrier, Y. Takakura, L. Bigu, F. Galland, and V. DeVlaminck, "Target detection with a liquid crystal-based passive stokes polarimeter," *Appl. Opt.*, vol. 43(2), pp. 274–282, 2004.

[5] V. Thilak, D. G. Voelz, and C. D. Creusere, "Estimating the complex index of refraction and view angle of an object using multiple polarization measurements," *Proc. Fortieth Asilomar Conf. Signals, Systems and Computers*, pp. 1067–1071, 2006.

[6] R. O. Duda, P. E. Hart, and D. G. Stork 2nd Ed., *Pattern Classification*, Wiley Interscience, New York, 2001.

[7] R. G. Priest and S. R. Meier, "Polarimetric microfacet scattering theory with applications to absorptive and reflective surfaces," *Opt. Eng.*, vol. 41(5), pp. 988–993, 2002.

[8] J. R. Shell II, *Polarimetric Remote Sensing in the Visible to Near Infrared*, Ph.D. dissertation, Rochester Institute of Technology, 2005.

[9] S. Damarla, *Automation and testing of an imaging polarimeter*, M.S. thesis, Electrical and Computer Engineering, New Mexico State University, 2006.

[10] "Luxpop," http://www.luxpop.com/.